Methods for phase noise mitigation for DFT-S-OFDM waveforms

METHODS FOR PHASE NOISE MITIGATION FOR DFT-S-OFDM WAVEFORMS

Ville Syrjälä, Toni Levanen and Mikko Valkama

Dept. of Electronics and Communications Eng., Tampere University of Technology, Finland
E-mail: ville.syrjala@tut.fi

ABSTRACT

This paper addresses the problem of phase noise mitigation in communications links utilizing DFT-S-OFDM waveforms. The paper discusses use of two different pilot configurations to do the compensation of the common phase error part of the phase noise. The pilot configurations are inserting pilots as logical symbols before the DFT spreading and inserting frequency domain pilots as subcarriers as in OFDM waveforms. Then, based on the former pilot configuration, a computationally efficient intercarrier interference compensation algorithm is proposed. The pilot configurations and techniques are evaluated in terms of peak-to-average power ratio and phase noise mitigation performance with realistic numerology in numerical simulations.

Index Terms—DFT-S-OFDM, 5G, cm-wave, phase noise, enhancing digital signal processing.

1. INTRODUCTION

VARIOUS waveforms, including numerous forms of Fourier transform spread orthogonal frequency division multiplexing (DFT-S-OFDM), have been proposed for the 5th generation (5G) mobile networks [1], [2], [3], [4], [5]. Even though the DFT-S-OFDM signal is practically a single carrier signal, it is still very sensitive to radio frequency (RF) impairments such as phase noise. This includes the common-phase-error (CPE) and intercarrier interference (ICI) effects of the phase noise, and even though the effects are observed a bit differently than in OFDM [6], we use similar terminology as in OFDM for simplicity. The CPE term in general denotes the average effect of the phase noise during a DFT-S-OFDM symbol and ICI denotes the excess phase error without the average. ICI observed in the frequency domain is due to the time varying nature of the phase noise during one FFT window.

In the literature, the phase noise estimation has not received wide attention for DFT-S-OFDM [6], [7], since in practice phase noise level is controlled by using good enough oscillators. This approach gets more and more challenging, as the carrier frequencies get higher and higher to cm and mm waves in 5G [8], [9], [10]. Unlike in OFDM or single carrier signal, in the DFT-S-OFDM, pilots can be inserted in two ways: 1) inserting pilots as

logical symbols before the DFT spreading, or 2) inserting the pilots as subcarriers as in OFDM, which potentially increases the PAPR. In this paper, both of the subcarrier insertion schemes are studied shortly in terms of PAPR and CPE mitigation. Also, an efficient algorithm is proposed for phase noise ICI estimation and mitigation, based on the first pilot insertion scheme. The phase noise can be estimated with a help of a cumulative sum filter over a coarse phase noise realization estimates at the logical pilot symbol locations. All the results are applicable for various forms of DFT-S-OFDM waveforms, including the zero tail [3] and guard interval [4] variants. The ICI compensation method also provides phase noise estimates for the guard interval or cyclic prefix part of the signal.

After this section, the outline of this paper is as follows. In Section 2, the used waveform and oscillator are presented. In Section 3, the used pilot insertion schemes and the corresponding ways to carry out CPE estimation are presented, and the ICI estimation and mitigation algorithm is proposed. The simulation results and performance analysis are given in Section 4 and the work is concluded in Section 5.

2. NUMEROLOGY AND OSCILLATOR MODEL

2.1 DFT-S-OFDM Link Numerology

The used numerology is based on those proposed for cm-wave communications in [8], [9] and [10]. We use FFT size of 2048 so that 1280 of the centermost FFT-bins, excluding the DC-bin, are used for transmission. 60 kHz subcarrier spacing is used, so the effective bandwidth is 80 MHz. CP size is set to 115. We also use a similar subframe structure as introduced in [10], and assume that the third symbol in the subframe is a data demodulation reference symbol (DMRS) used to estimate the channel. This channel estimate is then used to equalize all the 11 data DFT-S-OFDM symbols per subframe. This kind of frontloaded DRMS design leads to sub-optimal CPE compensation by the channel equalization and therefore also per data symbols CPE compensation is required.

2.2 Oscillator Model

The used oscillator model is based on the data sheet of a current state of the art phase-locked loop (PLL) type oscillator in [11]. Based on the past oscillator development, it is our educated guess
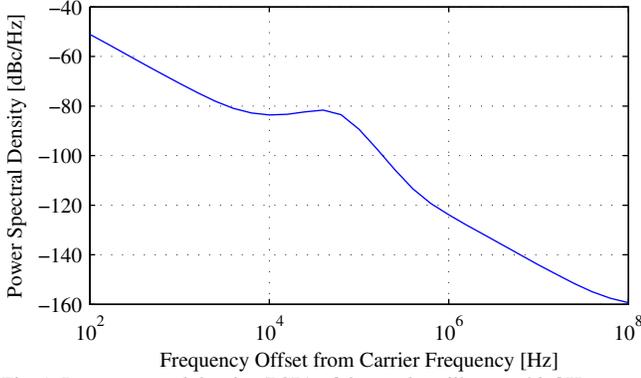
Fig. 1. Power spectral density (PSD) of the used oscillator at 28 GHz centre frequency.
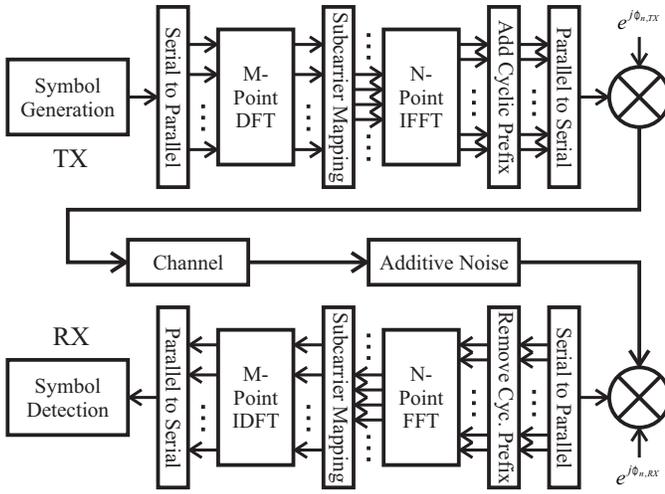

Fig. 2. DFT-S-OFDM link corrupted by transmitter and receiver phase noises, channel and additive noise.

that this level of oscillator quality represents the quality of oscillators in mobile devices at the time of 5G implementation. The spectrum of the used oscillator at 28 GHz center frequency is depicted in Fig. 1.

3. PILOT INSERTION SCHEMES AND PHASE NOISE MITIGATION

The DFT-S-OFDM waveform is generated and demodulated as depicted in Fig. 2. Notice that the *M*-point DFT spreading and inverse DFT (IDFT) despreading functions are denoted clearly as DFT and IDFT, even though they can be computed with the efficient FFT algorithm. The *N*-point OFDM modulation and demodulation are denoted by IFFT and FFT, for clarity. This terminology is used in this paper from now on.

3.1 Inserting Pilots before DFT Spreading

Inserting the pilot symbols before DFT spreading has benefits because the pilots are transmitted similarly to the actual data. The pilots do not therefore affect the properties of the DFT-S-OFDM waveform, such as low PAPR. At the received after the final stage of the DFT-S-OFDM demodulation, namely after the IDFT, the pilots act similarly as time-domain pilots, but at a lower sampling frequency than in the transmitted signal. The sampling frequency is *M/N* times the baseband sampling frequency of the signal before the IDFT.

After the IDFT, the CPE term of the phase noise is not really common phase error anymore from the modulated symbols perspective, as it is for the waveform samples before the IDFT. It is actually the average phase shift due to phase noise over the duration of all the symbols. The CPE term can therefore be estimated by estimating the average phase shifts over the pilot symbols after multiplication with the conjugated ideal pilot symbol values. The mitigation is done by using the estimated average phase error as a common phase derotation for all the symbols during the DFT-S-OFDM symbol. This corresponds to removing the CPE in OFDM, as CPE is also the average rotation due to phase noise during an OFDM symbol.

Notice that if DFT-S-OFDM is used as a multiple access scheme, the ICI causes also inter-user interference [6]. Even though this paper focuses on a single-user case, the results are generalizable for multiple access schemes as well.

3.2 Inserting Pilots after DFT Spreading

Inserting the pilot symbols after the DFT spreading result in similar type of pilots that are used in OFDM. This is why we use a term subcarrier pilot symbol. They can be used, e.g., in channel estimation similarly as in OFDM. However, inserting the pilot subcarriers increases the PAPR, as the resulting waveform gets more properties of an OFDM waveform.

Because the CPE part of the phase noise can already be addressed prior the IDFT, namely similarly as in OFDM, each pilot subcarrier symbol holds the CPE information in it. Therefore, after the channel estimation and equalization, the CPE estimation can simply be done by taking the average rotation over each of the pilot subcarriers after multiplying them by the conjugate of the ideal pilot subcarrier values.

Notice that from ICI point of view, this approach is a bit different than when the pilots are inserted before the DFT spreading. Phase noise spreads the energy of each of these subcarrier pilots as in OFDM, so energy of each of the pilots spreads on top of the data part of the signal in exactly the same way as in OFDM.

3.3 ICI Estimation if Pilots Are Inserted before DFT Spreading

In the ICI compensation algorithm proposed here, the estimation of the ICI part of the phase noise is carried out by the help of the pilot symbols after the IDFT at the receiver. At the transmitter upconversion and receiver downconversion, the phase noise affects the time-domain pilots directly. At the receiver before FFT, each FFT input sample is affected by the phase noise at the sampling frequency Nf_{sc}, where f_{sc} is the subcarrier spacing. After the *N*-point FFT and *M*-point IDFT, the same phase noise process still affect the received symbols at slower sampling rate Mf_{sc}.

Simplified model of our symbols stream with effective phase noise, s_n^{PN}, can be denoted by

$$s_n^{PN} = s_n e^{j\phi_n} + \gamma_n, \qquad (1)$$

where s_n is the transmitted symbols stream, ϕ_n is the combined effective phase error stemming from the transmitter and receiver phase noises, and γ_n includes all the noise components, also those stemming from the fact that the signal propagates through a multipath channel after being affected by the transmitter phase noise. Notice that the term ϕ_n does not include all the effects of phase noise, as the signal has gone through the channel, and the channel estimation and equalization. This form is simplified form and includes only the main effect of the combined transmitter and receiver phase noises. Weather this is reasonable or not is proven with the numerical simulation, where phase noise effect is handled without such simplifications.

Now, from (1) it stems that we can directly use evenly allocated pilot symbols to get a crude estimates of the phase noise at the time moments of the pilot symbols. It should be noted thought that the noise term γ_n is very significant, and the result of just multiplying the samples s_n^{PN} with the convolution of the pilot symbols would result in useless phase noise estimate. To combat the effect of the noise, we use cumulative sum filter over adjacent phase noise estimates, and even over adjacent DFT-S-OFDM symbols to get the estimates at the symbols boundaries. We first compute the crude estimates for the phase noise complex exponentials at the times of the pilot symbols as

$$\varepsilon_n = e^{j\hat{\phi}_n} = s_n^{PN} s_n^*, \quad n \in S_p, \qquad (2)$$

where S_p is the set of pilot indices, and the values of s_n^* are therefore known when $n \in S_p$. At this point the phase information could be forced to unit circle. Instead, we keep the amplitude information obtained from the received signal because it provides a good estimate of the reliability of each pilot symbols and automatically weights more reliable pilots in the filtering process. Then, the estimate vector $\varepsilon_n, n \in S_p$ is zero-padded, so that we have 1280 samples per DFT-S-OFDM symbol. The resulting zeros-padded signal is denoted by ε_n^{ZP}. This vector has crude estimates of the phase noise at the same time moments as the pilot symbols are allocated to the original symbol stream. Then CP is added to this zero-padded signal symbol by symbol, and the resulting signal is fed to a cumulative sum filter. The filtering is multiplierless, so its computational complexity is very low. The length of the cumulative sum filter can be optimized, but it should be more than the separation between two adjacent phase noise estimates to work. Cumulative sum filtering practically does computationally very efficient lowpass filtering to the signal. Since practical phase noise process is always a strong lowpass signal in nature, the filter filters out most of the noise, and passes through a cleaner estimate of the phase noise complex exponential. Since we know that the result should be pure complex exponential due to the nature of the phase error, in the end we force the amplitude of the estimate to unity, and obtain our final phase noise estimate.

This whole phase noise estimation process is computationally very efficient, as it only requires complex multiplication for the pilot symbols, cumulative summing of the signal where most of the elements are zeros[1], and forcing the amplitude of each phase noise complex exponential estimate to unity. Then the demodulated symbols are multiplied by the conjugates of the estimates of the phase noise complex exponential to mitigate the phase noise in time domain.

4. SIMULATIONS

4.1 Description of Simulator and Simulation Parameters

In the simulations, numerology and oscillator presented in the Section II is used. First, DFT-S-OFDM signal is generated from a stream of 64QAM modulated symbols following the process depicted in Fig. 2. Eight pseudorandom 64QAM modulated data pilots per DFT-S-OFDM symbol are added. If they are added before the DFT spreading, they are allocated equally spaced within the data stream. If they are added after the DFT spreading, they are allocated as equally spaced subcarriers. Then, the transmitter phase noise is modelled. After the transmitter phase noise, a channel is modelled as a tapped delay line. The power delay profile follows the ITU-R Urban Microcell Non Line-of-Sight (UMi NLoS) channel when the multipath channel is present, or the channel is just flat, if additive white Gaussian noise (AWGN) channel case is evaluated. After the channel, AWGN is generated to get the desired signal-to-noise ratio (SNR). At the receiver, first, received phase noise is modelled, followed by the DFT-S-OFDM demodulation depicted in Fig. 2. After this the phase noise estimation and mitigation techniques are applied case by case. Each result point in the simulation is generated as an average BER is computed over 5000 random channel realizations realizations. The carrier frequency is set to 28 GHz, so the transmitter and receiver phase noise PSDs follow the curve depicted in Fig. 1. The length of the used cumulative sum filter for the proposed phase noise ICI compensation algorithm is 1000. Because most of the cumulatively summed samples are zeros, this only results in very low amount, around 40, summations during the whole DFT-S-OFDM symbol. The value 1000 was selected empirically.

In the simulation results, cases are denoted in the legend of the figure as follows: 1) 'Ideal CPE' refers to a case when the DC-bin of the phase noise is ideally known, and it is used in the phase noise mitigation, 2) 'CPE Est. 1' refers to the case where CPE is estimated in a case when pilots are inserted before the DFT spreading and 3) 'CPE Est. 2' refers to the case where CPE is estimated when the pilots are inserted after the DFT spreading. Finally, 4) 'Pilot Int.' refers to the phase noise ICI estimation and mitigation scheme proposed in this paper.

---

[1] Notice that as the most of the elements that are cumulatively summed are zeros, the actual implementation can be done with a slower rate cumulative summer that updates the value of the phase noise estimate only a few times during a DFT-S-OFDM symbol.
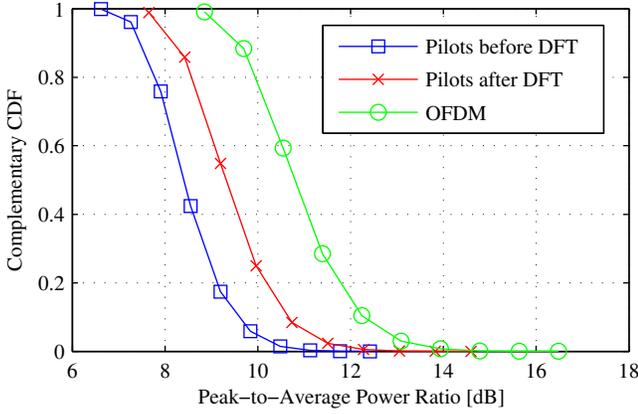
Fig. 3. Complementary cumulative distribution function (CCDF) given for peak-to-average power ratio (PAPR). 64QAM symbols are used.
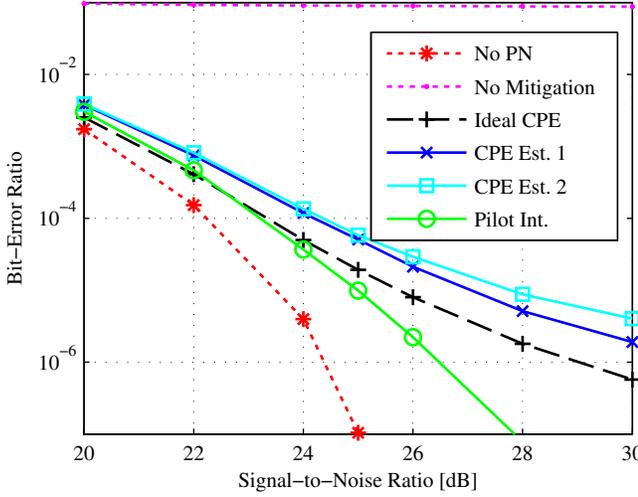

Fig. 4. Bit-error ratio evaluated as a function of signal-to-noise ratio. Additive white Gaussian noise channel is used.
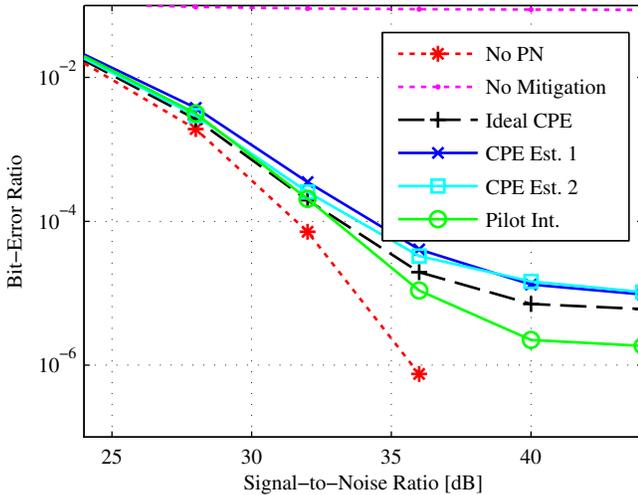

Fig. 5. Bit-error ratio evaluated as a function of signal-to-noise ratio. ITU-R UMi NLoS multipath channel is used.

To our understanding the only reference algorithm able to estimate the phase noise in this type of setup is the one proposed in [6]. It was not included in the performance comparisons, because the complexity of the algorithm is on totally different level, thousands of times more complex, due to burdensome reconstruction of the received signal and iterations. This makes the algorithm rather unrealistic for practical implementation. We currently work on lowering the complexity of the algorithm in [6].

4.2 Simulation Results and Analysis

In Fig. 3, PAPR of the different pilot insertion schemes are compared to the PAPR of plain OFDM. The PAPR is computed for 20000 DFT-S-OFDM symbols and complementary cumulative density function (CCDF) is estimated from those realizations. Clearly the clean DFT-S-OFDM waveform where the pilots are inserted before the DFT spreading gives the lowest PAPR. When the pilots are inserted as subcarrier after the DFT spreading, the PAPR intuitively increases, but with 8 pilots stays clearly below the PAPR of a plain OFDM waveform.

Computed bit-error ratios (BER) for the flat AWGN channel and for ITU-R UMi NLoS multipath channel are given in Fig. 4 and Fig. 5, respectively. From the both of the figures we can conclude that when the phase noise is the dominating error, inserting the pilots before the DFT spreading provides better results than when adding the pilots after the DFT spreading. This is logical as each pilot provides estimate of a single realization of the phase noise process at the time of the pilot. Averaging the phase noise realization over these pilots is accurate when the phase noise is relatively powerful. However, when the pilot subcarriers are inserted after the DFT spreading, each subcarrier has the full phase noise effect during the DFT-S-OFDM symbol in it. Therefore estimating the average rotation of these is relatively robust when the other noise components are relatively powerful, at low SNRs.

From Fig. 4 and Fig. 5 we can see that the proposed phase noise ICI compensation algorithm provides very good overall performance. At higher SNR levels with multipath channel, it is able to provide even a decade drop in BER, and around 10 dB improvement over the CPE estimation cases. The flat channel case shows, that the all-around performance compared to the no phase noise curve stays less than 3 dB away. Also, in the multipath channel case, the SNR degradation due to phase noise stays at reasonable level, e.g., at around 3 dB even at very low BER of 10e-5, when the proposed algorithm is used.

5. CONCLUSION

Various forms of DFT-S-OFDM waveforms have been proposed to be utilized in 5G networks. In DFT-S-OFDM, pilots can be allocated before or after the DFT spreading of the transmitted symbols. Both the cases allow common phase error part of the phase noise to be estimated with quite similar accuracy. However, allocating the pilots after the DFT spreading increases the PAPR significantly. The intercarrier interference estimation and mitigation technique based on the pilots allocated before the DFT spreading was also proposed in this paper. The performance of the algorithm was proven to be very good, as it was able to improve the SNR even in order of 10 dB for practical multipath channel case at low BER levels.

REFERENCES

[1] G. Wunder, *et al.*, "5GNOW: non-orthogonal asynchronous waveforms for future mobile applications," *IEEE Communications Magazine*, vol. 52, no. 2, pp. 97-105, Feb. 2014.

[2] P. Banelli, S. Buzzi, G. Colavolpe, A. Modenini, F. Rusek, and A. Ugolini, "Modulation formats and waveforms for 5G networks: Who will be the heir of OFDM?," *IEEE Signal Processing Magazine*, vol. 31, no. 6, pp. 80-93, Nov. 2014.

[3] G. Berardinelli, *et al.*, "On the potential of zero-tail DFT-spread-OFDM in 5G networks," in *Proc. IEEE Vehicualr Technology Conference 2014-Fall*, Vancouver, Canada, Sep. 2014.

[4] U. Kumar, C. Ibars, A. Bhorkar, H. Jung, "A waveform for 5G: Guard interval DFT-s-OFDM," in *Proc. IEEE Globecom Workshops 2015*, San Diego, CA, Dec. 2015.

[5] G. Berardinelli, K. Pajukoski, E. Lähetkangas, R. Wichman, O. Tirkkonen, and P. Mogensen, "On the potential of OFDM enhancements as 5G waveforms," in *Proc. IEEE Vehicular Technology Conference 2014-Spring*, Seoul, South Korea, May 2014.

[6] V. Syrjälä, "Modelling and Practical Iterative Mitigation of Phase Noise in SC-FDMA," In *Proc. IEEE Int. Symp. on Personal, Indoor and Mobile Radio Commun. 2012*, Sydney, Australia, Sep. 2012.

[7] S. B. Ryu, J. Kim, H.G. Ryu, and Y. Li, "PNS algorithm for the SCFDMA communications system with phase noise," in *Proc. IFIP Internation Conference on Wireless and Optical Communications Networks 2009*, Cairo, Egypt, Apr. 2009.

[8] P. Mogensen, K. Pajukoski, E. Tiirola, and E. Lähetkangas, "5G small cell optimized radio design," in *Proc. IEEE Global Communications Conference 2013 (Globecom 2013) Workshops*, Atlanta, GA, Dec. 2013.

[9] P. Mogensen *et al.*, "Centimeter-wave concept for 5G ultra-dense small cells," in *Proc. IEEE Vehicular Technology Conference 2014-Spring*, Seoul, South Korea, May 2014.

[10] E. Lähetkangas, K. Pajukoski, J. Vihriälä, and E. Tiirola, "On the flexible 5G dense deployment air interface for mobile broadband," in *Proc. International Conference on 5G for Ubiquitous Connectivity*, Akaslompolo, Finland, Nov. 2014.

[11] Hittite HMC704LP4E, http://www.analog.com/media/en/technical-documentation/data-sheets/hmc704.pdf

[12] International Telecommunication Union Radiocommunication Sector (ITU-R), "Report ITU-R M.2135-1: Guidelines for evaluation of radio interference technologies for IMT-Advanced," Dec. 2009.